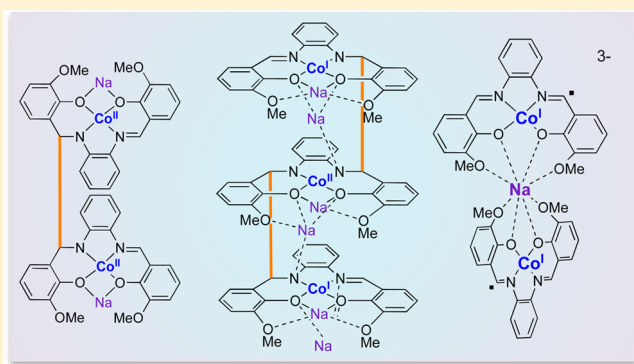


Ligand and Metal Based Multielectron Redox Chemistry of Cobalt Supported by Tetradentate Schiff Bases

Julie Andrez,[†] Valentin Guidal,[‡] Rosario Scopelliti,[†] Jacques Pécaut,[‡] Serge Gambarelli,[‡] and Marinella Mazzanti^{*,†,§}[†]Institut des Sciences et Ingénierie Chimiques Ecole Polytechnique Fédérale de Lausanne (EPFL), 1015 Lausanne, Switzerland[‡]Univ. Grenoble Alpes, CEA, CNRS, INAC, SYMMES, F-38000 Grenoble, France

S Supporting Information

ABSTRACT: We have investigated the influence of bound cations on the reduction of cobalt complexes of redox active ligands and explored the reactivity of reduced species with CO₂. The one electron reduction of [Co^{II}(^Rsalophen)] with alkali metals (M = Li, Na, K) leads to either ligand-centered or metal-centered reduction depending on the alkali ion. It affords either the [Co^I(^Rsalophen)K] complexes or the [Co^{II}₂(bis-salophen)M₂] (M = Li, Na) dimers that are present in solution in equilibrium with the respective [Co^I(salophen)-M] complexes. The two electron reduction of [Co^{II}(^{OMe}salophen)] results in both ligand centered and metal centered reduction affording the Co(I)–Co(II)–Co(I) [Co₃(tris-^{OMe}salophen)Na₆(THF)₆], **6** complex supported by a bridging deca-anionic tris-^{OMe}salophen¹⁰⁻ ligand where three ^{OMe}salophen units are connected by two C–C bonds. Removal of the Na ion from **6** leads to a redistribution of the electrons affording the complex [(Co(^{OMe}salophen))₂Na][Na(cryptand)]₃, **7**. The EPR spectrum of **7** suggests the presence of a Co(I) bound to a radical anionic ligand. Dissolution of **7** in pyridine leads to the isolation of [Co^I₂(bis-^{OMe}salophen)Na₂Py₄][Na(cryptand)]₂, **8**. Complex **6** reacts with ambient CO₂ leading to multiple CO₂ reduction products. The product of CO₂ addition to the ^{OMe}salophen ligand, [Co(^{OMe}salophen-CO₂)Na]₂[Na(cryptand)]₂, **9**, was isolated but CO₃²⁻ formation in 53% yield was also detected. Thus, the electrons stored in the reversible C–C bonds may be used for the transformation of carbon dioxide.



■ INTRODUCTION

Multielectron redox processes play a key role in chemical and enzymatic transformations catalyzed by transition metals. An increasingly used strategy, both in d-block and f-block chemistry, for the design of complexes capable of multielectron transfer, involves the use of redox-active ligands.^{1–6} These ligands can be used to store and release electrons during substrate transformation, without a change in the metal oxidation state, and as such to enable novel reactivity.^{7–10} Notably, the excellent properties of bis(imino)pyridine as supporting ligands in catalytic and stoichiometric reactions mediated by first row transition metals have been interpreted in terms of their redox-active character.^{8,11–14} The redox-active behavior of ligands such as polypyridines or unsaturated azamacrocycles also plays a key role during electrocatalytic CO₂ reduction by metal complexes of these ligands impacting on reactivity and product selectivity.^{15–19} Other ligands with well identified redox-active behavior include amido-phenolates,²⁰ dipyrromethane,²¹ diazadienes,^{22–25} azopyridine,²⁶ bipyridine,^{27,28} phenanthroline,²⁹ terpyridine.³⁰

Redox events at the ligand may be accompanied by the formation of a new C–C bond^{29,31–34} that in some cases is reversible.^{29,31,32,35,36} Tetradentate Schiff bases can act as redox-

active ligands in complexes of d-block^{37–41} and f-block^{6,42,43} metals leading to intramolecular or intermolecular C–C bond formation. Moreover, reactivity studies suggest that the electrons stored in the C–C bond may become available for various chemical transformations including CO₂ fixation.³⁷ Schiff base complexes of cobalt have been reported to act as catalyst in the electrochemical reduction of CO₂,⁴⁴ and in hydrogen production,⁴⁵ but the role of ligand-based redox processes in these transformations has not been elucidated.

The chemical monoelectronic reduction of the [Co^{II}(^Rsalophen)] (R = H and OMe) was shown not to affect the metal center but to afford the reduction of the imine group and C–C formation.³⁷ The resulting complex was reported to bind reversibly carbon dioxide.³⁷ Although the structure of the carbon dioxide adduct was not characterized, it was proposed to be very similar to that of the complex [Co^I(^Rsalen)K(CO₂)].⁴⁶ The latter complex forms reversibly from the reaction of CO₂ with the bimetallic Co(I) complex [Co^I(^Rsalen)K] obtained from the reduction of the Schiff base complex [Co^{II}(^Rsalen)] (R = H, Et and nPr) with K.⁴⁶ This reaction was the first example

Received: April 10, 2017



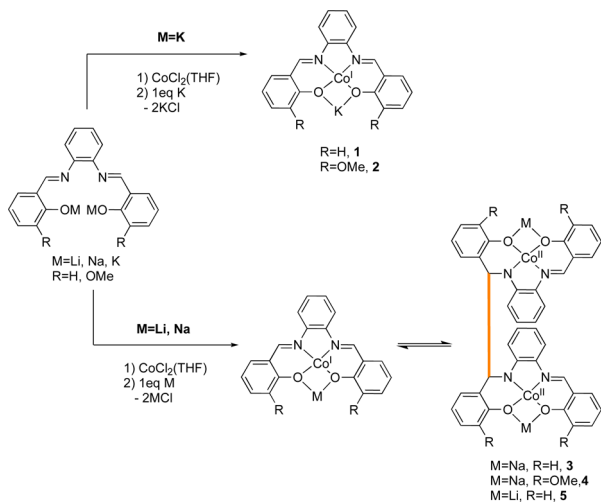
of cooperative binding of carbon dioxide by a heterobimetallic complex. Multimetallic cooperative binding is thought to play a key role in electrocatalytic reduction of carbon dioxide and in its biological transformation,^{47–49} but examples of carbon dioxide reduction at molecular heterobimetallic complexes remain very rare up to date.^{50–54}

Recent studies from Bart and co-workers have shown that subtle variation of the donor properties of coligands structure in uranium complexes of bis(imino)pyridine leads to drastic changes in the distribution of the charge in these complexes and in their reactivity.⁵⁵ In contrast the possible effect of the presence and nature of bound counterions on the electronic structure of complexes of redox active ligands has not been investigated. The heterobimetallic $[\text{Co}^{\text{I}}(\text{salophen})\text{M}]$ ($\text{M} = \text{Li}, \text{Na}, \text{K}$) complex is an ideal candidate to investigate how bound cations affect the redox chemistry in metal complexes of redox active ligands. Here we show that the presence of bound cations and the nature of the cation result in dramatic changes in the structure of the reduced species.

RESULTS AND DISCUSSION

One Electron Reduction of $\text{Co}^{\text{II}}(\text{salophen})$ Complexes by Alkali Metals. The reduction of the $\text{Co}(\text{II})$ complexes $[\text{Co}(\text{salophen})]$ and $[\text{Co}^{\text{OMe}}(\text{salophen})]$ with one equivalent of potassium metal in THF affords the polymeric complex $[\text{Co}(\text{salophen})\text{K}(\text{THF})]_n$ **1** and the monomeric complex $[\text{Co}^{\text{OMe}}(\text{salophen})\text{K}(\text{THF})]$, **2** (Scheme 1).

Scheme 1. Reduction of $[\text{Co}^{\text{R}}(\text{salophen})]$ ($\text{R} = \text{H}, \text{OMe}$) with Alkali Metals



The solid state structure of **1** determined by X-ray diffraction (Figure 1) shows the presence of a heterobimetallic CoK complex where the phenolate oxygen atoms bind both the Co and the K cations. Each K ion binds two THF molecules, two oxygen atoms from one $\text{Co}(\text{salophen})$ moiety and two oxygen atoms from another $\text{Co}(\text{salophen})$ moiety resulting in a polymeric structure. The Co ion is tetracoordinated by the two oxygen and two nitrogen atoms of the salophen ligand with a square planar geometry. The structure of complex **1** is similar to that previously reported for the polymeric complex $[\text{Co}(\text{salen})\text{Na}(\text{THF})]_n$ prepared by reduction of $[\text{Co}(\text{salen})]$ with sodium metal.^{56,57} The mean $\text{Co}-\text{O}$ (1.90(1) Å and $\text{Co}-\text{N}$ distances (1.829(8) Å) (selected bond distances for all complexes are summarized in Table 1) are comparable to those

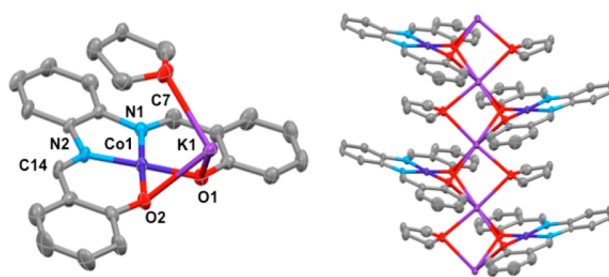


Figure 1. ORTEP of the $[\text{Co}(\text{salophen})\text{K}(\text{THF})]_n$ **1** (right) polymer and of the $[\text{Co}(\text{salophen})\text{K}(\text{THF})]$ unit (left). Ellipsoids at 50%. Carbon atoms in gray, hydrogen atoms omitted for clarity.

Table 1. Average Bond Distances in Reduced $\text{Co}(\text{salophen})$ Complexes

	$\text{Co}-\text{N}_{\text{imino}}$	$\text{Co}-\text{N}_{\text{amido}}$	$\text{Co}-\text{O}$	$\text{C}-\text{N}_{\text{imino}}$	$\text{C}-\text{N}_{\text{amido}}$
1	1.829(8)	/	1.90(1)	1.303(3)	/
2	1.833(6)	/	1.884(8)	1.327(4)	/
3	1.852(5)	1.824(5)	1.87(3)	1.306(8)	1.464(7)
5	1.892(4)	1.875(4)	1.916(5)	1.298(6)	1.449(5)
6	1.830(6)	1.857(4)	1.90(3)	1.359(8)	1.457(1)
7	1.84(1)	/	1.86(3)	1.34(2)	/

found in the $[\text{Co}(\text{salen})\text{Na}(\text{THF})]_n$ polymer ($\text{Co}-\text{O} = 1.899(3)$ Å and $\text{Co}-\text{N} = 1.82(1)$ Å). A lengthening of the $\text{Co}-\text{O}$ distances and a shortening of the $\text{Co}-\text{N}$ distances compared to those found in $[\text{Co}(\text{salophen})]$ ($\text{Co}-\text{O} = 1.843(4)$ Å and $\text{Co}-\text{N} = 1.873(4)$ Å) is observed.⁵⁸ The lengthening of the $\text{Co}-\text{O}$ distances is due to the K^+ binding, while the shortening of the $\text{Co}-\text{N}$ bond is consistent with the presence of cobalt in a lower oxidation state.⁵⁷

Crystals of $[\text{Co}^{\text{OMe}}(\text{salophen})\text{K}]$ were obtained by slow diffusion of DIPE into a THF solution of complex **2**. The solid structure of **2** (Figure 2), shows the presence of a

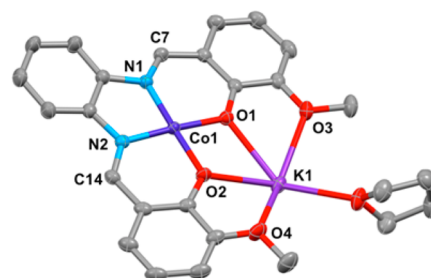


Figure 2. ORTEP of $[\text{Co}^{\text{OMe}}(\text{salophen})\text{K}(\text{THF})]_2$ **2**. Ellipsoids at 50%. Carbon atoms in gray. Hydrogen atoms omitted for clarity.

tetracoordinate cobalt ion in the O_2N_2 pocket of the ligand with a square planar geometry. The average $\text{Co}-\text{O}$ and $\text{Co}-\text{N}$ distances are 1.884(8) Å and 1.833(6) Å respectively and are in the range of those found in complex **1**. The two distances $\text{C}7-\text{N}1$ and $\text{C}14-\text{N}2$ (1.329(2) Å and 1.324(2) Å) are in agreement with the presence of $\text{C}=\text{N}$ double bonds. The potassium counterion binds the four oxygen atoms of the ligand slightly below the oxygen atoms plane (0.65 Å). A THF molecule completes its coordination sphere. The methoxy substituents of the OMe -salophen ligand provide a binding pocket for the potassium cation thus preventing polymerization.

The structure of complexes **1** and **2** differs from the solid state structures previously reported for the compound obtained

from the reduction of $[\text{Co}(\text{salophen})]$ and $[\text{Co}^{\text{OMe}}(\text{salophen})]$ with sodium metal.³⁷ Notably, the reduction of $[\text{Co}(\text{salophen})]$ and $[\text{Co}^{\text{OMe}}(\text{salophen})]$ by sodium does not lead to the reduction of the Co(II) center to Co(I), but to the reduction of the imino function of the ligand yielding the dimeric complexes of cobalt(II) $[\text{Co}_2(\text{bis-salophen})\text{Na}_2(\text{THF})_6]$, **3** $[\text{Co}_2(\text{bis-OMe-salophen})\text{Na}_2(\text{THF})_4]$, **4** (Scheme 1). These complexes contain the reduced hexa-anionic bis-salophen ligands arising from the formation of a C–C bond between two reduced imino carbons of two different salophen units.

The difference in the molecular structure of the compounds obtained from the reduction of $[\text{Co}(\text{salophen})]$ and $[\text{Co}^{\text{OMe}}(\text{salophen})]$ with K and Na, indicates that the nature of the alkali ion has an important effect on the outcome of the reduction. While in the presence of potassium the reduction occurs on the metal, in the presence of sodium it occurs on the ligand.

In order to gain more information on these compounds we have investigated and compared the solution structure of complexes **1** and **2** with that of the previously reported $[\text{Co}_2(\text{bis-salophen})\text{Na}_2(\text{THF})_6]$ complex. The $[\text{Co}_2(\text{bis-salophen})\text{Na}_2(\text{THF})_6]$, **3** and $[\text{Co}_2(\text{bis-OMe-salophen})\text{Na}_2(\text{THF})_4]$, **4** complexes were prepared using a modified literature procedure.³⁷ Notably, in the published procedure the dimeric complexes **3** and **4** were prepared by reacting $[\text{Co}(\text{salophen})]$ and $[\text{Co}^{\text{OMe}}(\text{salophen})]$ with an excess sodium (1.5 to 2.5 equiv) for 4 h. Considering that excess sodium can lead to further reduction (see following sections) we prepared the complexes **3** and **4** by reacting the Co(II) precursors with one equivalent of sodium for 24 h.

The proton NMR spectra of **1** and **2** in deuterated THF (up to the solubility limit) show the presence of only one set of seven signals in the diamagnetic region between 6.0 and 10.4 ppm in agreement with the presence of C_{2v} symmetric solution species containing a diamagnetic square planar Co(I) d^8 complex. The X band (9.6473 GHz) EPR spectrum of a 10 mM solution of **1** in THF/DIPE 4:1 at 10.1 K does not show any signal in agreement with the presence of a square planar Co(I) d^8 complex.

The ^1H NMR spectrum in THF at 298 K of the complex **3** prepared “in situ” by reduction of a 0.353 M solution of $[\text{Co}(\text{salophen})]$ with one equivalent of sodium metal shows a significantly more complex pattern compared to the ^1H spectrum of **1** (Figure 3). The presence of two sets of signals,

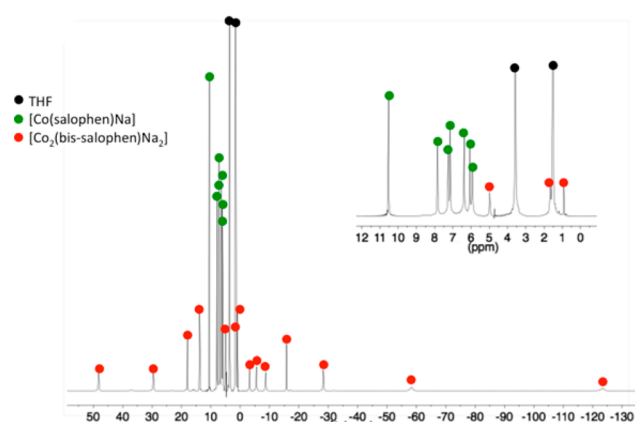


Figure 3. ^1H RMN (298 K, 400 MHz) spectrum in $\text{THF-}d_8$ of a 0.353 M solution of $[\text{Co}(\text{salophen})]$ reacted with one equivalent of Na.

one in the diamagnetic region and one in the paramagnetic region, is clearly identified. The first set of seven signals in the 6.0–10.6 ppm region is similar to that found in the ^1H NMR spectrum of **1** (see Supporting Information) and accordingly suggests the presence of a square planar Co(I) d^8 complex of analogous $[\text{Co}(\text{salophen})\text{Na}(\text{THF})]$ formula. A second set of 14 signals is also found in the paramagnetic region between 50 and –130 ppm. These signals are in agreement with the presence in solution of the dimeric Co(II) complex $[\text{Co}_2(\text{bis-salophen})\text{Na}_2(\text{THF})_6]$.

Proton NMR studies of this system (Figure 4) show that the ratio of Co(II) versus Co(I) species in solution changes with

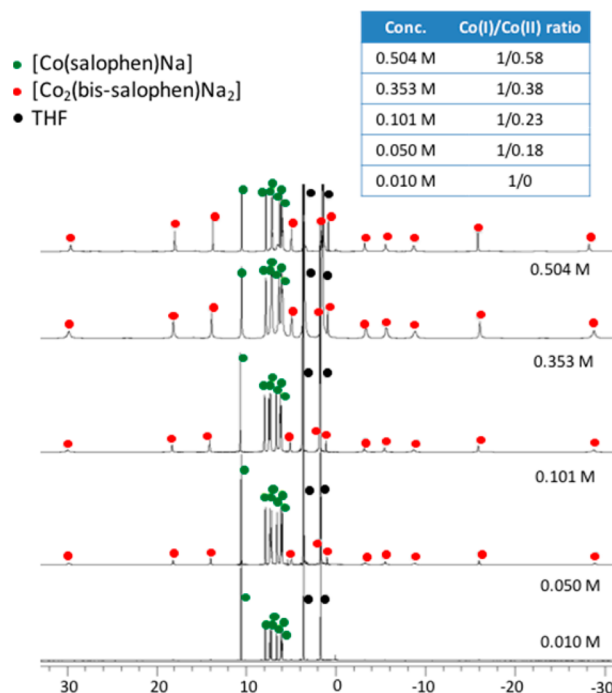


Figure 4. Zoom of the ^1H NMR spectra (298 K, 400 MHz) (between 32 and –30 ppm) in $\text{THF-}d_8$ of complex **3** at variable concentrations.

the concentration in agreement with the presence of an equilibrium between the monomeric Co(I) complex and the dimeric Co(II) complex. Notably, for starting concentrations of the $[\text{Co}(\text{salophen})]$ complex equal to or lower than 10 mM only the set of signals assigned to the monomeric Co(I) complex is observed. Due to the low solubility of $[\text{Co}_2(\text{bis-salophen})\text{Na}_2(\text{THF})_6]$ it was not possible to attain concentrations where only this complex is present in solution. The measurement of the diffusion coefficients by Pulsed-Field Gradient Stimulated Echo (PFGSTE) NMR in $\text{THF-}d_8$ at 298 K for the two species ($D_{\text{Co(I)}} = 5.92 \cdot 10^{-10} \text{ m}^2/\text{s}$ and $D_{\text{Co(II)}} = 5.17 \cdot 10^{-10} \text{ m}^2/\text{s}$) is in agreement with the presence of a monomeric and a dimeric complex in solution. Finally the presence of the previously reported complex $[\text{Co}_2(\text{bis-salophen})\text{Na}_2]$ in the concentrated mixture was confirmed by X-ray diffraction of the crystallized product.

EPR studies were also carried out for 4/1 THF:DIPE solutions of the $[\text{Co}(\text{salophen})]$ complex and of its reduction products at different concentrations (Figure 5). The EPR spectrum of a 4/1 THF:DIPE solution of $[\text{Co}(\text{salophen})]$ shows a signal typical for low-spin square planar Co(II) complexes.⁵⁹ In spite of the broadening, a characteristic eight-line pattern arising from the interaction of the electronic spin with the

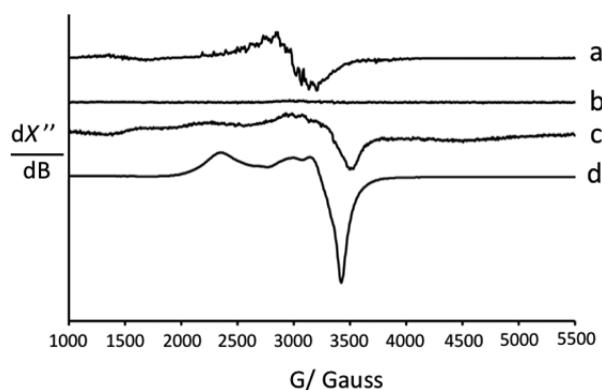


Figure 5. X-Band EPR spectra of 4:1 THF:DIPE solutions of (a) $[\text{Co}(\text{salophen})]$, 10 mM, (b) $[\text{Co}(\text{salophen})\text{Na}]$, 10 mM, (c) $[\text{Co}(\text{salophen})\text{Na}]/[\text{Co}_2(\text{bis-salophen})\text{Na}_2]$, 30 mM. (d) X-Band EPR spectra of isolated powders of $[\text{Co}_2(\text{bis-salophen})\text{Na}_2(\text{THF})_6]$ suspended in hexane.

cobalt nucleus ($I_{\text{Co}} = 7/2$) is unambiguously observed in the high field component. In order to measure the EPR of the complex **3** at different concentrations we prepared the complex in situ because its solubility is very low once it is crystallized. The EPR spectrum of the reaction mixture obtained after reduction of $[\text{Co}(\text{salophen})]$ with one equivalent sodium metal has been measured for 10 mM and 30 mM concentrations both at room temperature (no signal observed) and at 10 K after rapidly freezing the solutions prepared at room temperature.

No EPR signal is observed at 10 K for the frozen 10 mM solution in agreement with the only presence of the diamagnetic square-planar d^8 Co(I) complex $[\text{Co}(\text{salophen})\text{Na}]$ (Figure 5b). In contrast, the EPR spectrum of the frozen 30 mM solution shows (at 10 K) the presence of a complex anisotropic signal in agreement with the presence of several paramagnetic Co(II) species in solution (Figure 5c). The EPR spectrum obtained for powders of the complex $[\text{Co}_2(\text{bis-salophen})\text{Na}_2(\text{THF})_6]$ suspended in *n*-hexane is simpler and exhibit a pattern characteristic of an axial *g* tensor ($g_{\parallel} = 2.926$, $g_{\perp} = 2.012$) with no observable hyperfine coupling (Figure 5d). Upon close observation, this pattern can also be found in the previous spectrum (Figure 5c).

The results presented here are in agreement with the presence in solution of an equilibrium between a Co(I)-salophen and Co(II)-bis-salophen species (Scheme 1). The proposed radical intermediate containing a Co(II) bound to a reduced salophen ligand could not be clearly identified by EPR solution studies. We note that the equilibrium between the Co(II)/Co(I) species is reached immediately after the concentration adjustment. Moreover, the ratio Co(II)/Co(I) increases when the temperature is decreased. A variable temperature NMR study allows the determination of the thermodynamic parameters for the interconversion Co(II)/Co(I). The Van't Hoff analysis for this equilibrium leads to values of $\Delta H^0 = -5.4(1)$ kcal/mol and of $\Delta S^0 = -14(1)$ cal/mol/K. The value of ΔG^0 ($-1.2(1)$ kcal/mol) at 298 K is close to 0 kcal/mol indicating that the C–C bond formation is thermodynamically favored at room temperature but the bond dissociation energy is close to zero. Several examples of reversible C–C coupling with low dissociation energies (10–20 kcal mol $^{-1}$) have been reported in metal complexes^{29,60} and in sterically hindered organic compounds such as the Gomberg's dimer.⁶¹ However, the bonding dissociation energy measured

for this complex shows the presence of a very weak C–C bond with ΔG close to zero. Comparable values have only been found for a C–C bonded phenoxyl radical dimer (bond dissociation energy of 6.1(5) kcal mol $^{-1}$)⁶² and in the $[\text{Cp}^*\text{Yb}(\text{phen})]$ complex (bond dissociation energy of 8.1(2) kcal mol $^{-1}$).²⁹

In contrast to what observed for **3**, the proton NMR of the previously reported $[\text{Co}_2(\text{bis-OMe-salophen})\text{Na}_2(\text{THF})_4]$, **4** (prepared in situ by reduction of the $[\text{Co}(\text{OMe-salophen})]$ with one equivalent of sodium metal) shows the presence of only one set of 7 signals in the diamagnetic region in agreement with the presence in solution of the $[\text{Co}(\text{OMe-salophen})\text{Na}]$ complex. In this case dimerization is not detectable by proton NMR in solution up to the solubility limit (10 mM) of the complex but occurs in the solid state.

In order to further investigate the effect of the alkali ions we have also performed the reduction of the $[\text{Co}(\text{salophen})]$ complex with Li metal (Scheme 1). Proton NMR studies of the reaction mixture obtained from the reduction of the $[\text{Co}(\text{salophen})]$ complex with 1 equiv of Li metal show the presence of two sets of 7 and 14 signals that were assigned to a monomeric Co(I) $[\text{Co}(\text{salophen})\text{Li}(\text{THF})_x]$ complex and to a Co(II) dimeric complex $[\text{Co}_2(\text{bis-salophen})\text{Li}_2(\text{THF})_x]$. This suggests that the reduced complex behaves similarly in the presence of Na^+ and Li^+ cations. X-ray quality crystals of the dimeric complex $[\text{Co}_2(\text{bis-salophen})\text{Li}_2(\text{Py})_4]$, **5** were obtained by recrystallization of the reaction mixture in pyridine. The structure of **5** (Figure 6) shows the presence of a reduced hexa-

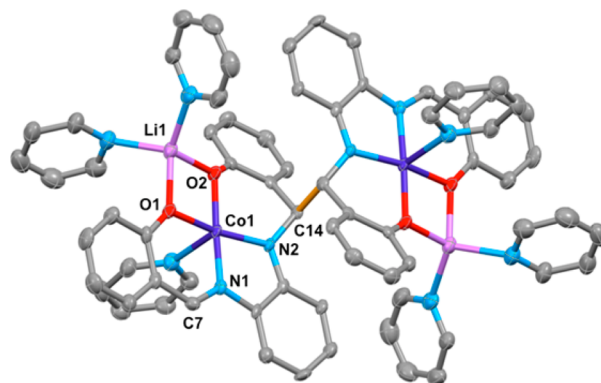


Figure 6. ORTEP of the structure of $[\text{Co}_2(\text{Py})_2(\text{bis-salophen})\text{Li}_2(\text{Py})_4]$, **5**. Ellipsoids at 50%. Carbon atoms in gray, C–C bond between reduced imino groups in orange, hydrogen atoms omitted for clarity.

anionic bis-salophen ligand resulting from the formation of a C–C bond (1.581(8) Å) between the two carbon atoms of the reduced imino groups from two different Co(salophen) units related by the symmetry center of the $P2_1/n$ space group. Each cobalt center is five coordinated by two oxygens and two nitrogens of the bis-salophen ligand and one pyridine nitrogen with a square pyramidal geometry. Each lithium cation is tetracoordinated by two oxygens of the bis-salophen ligand and two pyridine nitrogens with a tetrahedral geometry. Significantly different C–N distances are found for the imino (1.298(6) Å) and amido (1.449(5) Å) nitrogens in agreement with the presence of double and single bond, respectively.

A variable temperature NMR study was then performed to determine the thermodynamic parameters for the interconversion Co(II)/Co(I) in the presence of Li^+ (Figure 7). The Van't

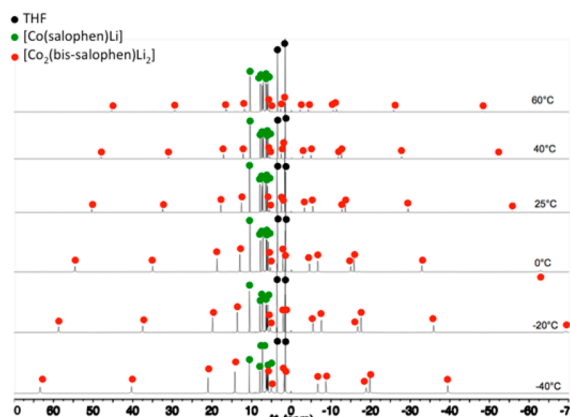


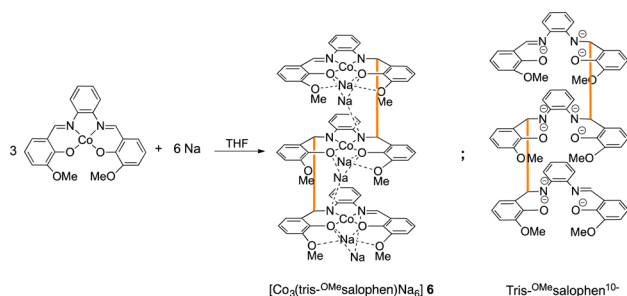
Figure 7. Variable temperature ^1H NMR spectra (400 MHz) from -40 to 60 $^\circ\text{C}$ of a 0.206 M solution in $\text{THF-}d_8$ of $[\text{Co}(\text{salophen})]$ reacted with one equivalent of Li .

Hoff analysis leads to values of $\Delta H^0 = -4.1(1)$ kcal/mol and of $\Delta S^0 = -11(1)$ cal/mol/K. The value of ΔG^0 (at 298 K) is of $-0.7(1)$ kcal/mol indicating once again that the C–C bond formation is thermodynamically favored at room temperature but the bond dissociation energy is close to zero.

These results show a very similar behavior for the heterobimetallic Co–M complexes of the salophen ligand for $M = \text{Na}$ or Li . In both cases Co(II) complexes containing a reduced ligand are isolated in the solid state, but in solution the species arising from metal-centered reduction and ligand-centered reduction are in equilibrium through reversible C–C bond formation. In contrast for $M = \text{K}$ only the Co(I) complex is formed both in THF solution and in the solid state.

Two Electron Reduction of the $[\text{Co}^{\text{OME}}\text{salophen}]$ Complex by Alkali Metals. Proton NMR studies show that the reduction of the Co(II) complexes $[\text{Co}(\text{salophen})]$ and $[\text{Co}^{\text{OME}}\text{salophen}]$ with two equivalents of potassium metal leads to the formation of further reduced products. Here we have further explored the products of the two-electron reduction of $[\text{Co}^{\text{OME}}\text{salophen}]$. The addition of 2 equiv of Na to a suspension of $[\text{Co}^{\text{OME}}\text{salophen}]$ complex leads to a green solution (Scheme 2). Crystals of the trimeric complex

Scheme 2. Two Electron Reduction of $[\text{Co}^{\text{OME}}\text{salophen}]$ (Left) and the Ligand $\text{Tris-}^{\text{OME}}\text{salophen}^{10-}$ (Right)



$[\text{Co}_3(\text{tris-}^{\text{OME}}\text{salophen})\text{Na}_6(\text{THF})_6]\cdot\text{hex}$, **6** $\cdot\text{hex}$, were obtained from the slow diffusion of hexane into a THF solution of **6** (Figure 8). The crystal structure of **6** shows that reduction has occurred both on the metal and on the imino groups of the ligand affording a $\text{Co(I)}\text{--Co(II)}\text{--Co(I)}$ complex supported by the deca-anionic $\text{tris-}^{\text{OME}}\text{salophen}^{10-}$ ligand. This ligand is formed from the coupling of three reduced $^{\text{OME}}\text{salophen}$

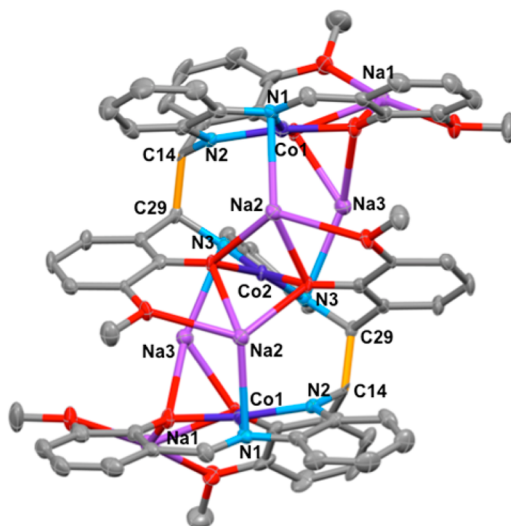


Figure 8. ORTEP of the structure of $[\text{Co}_3(\text{tris-}^{\text{OME}}\text{salophen})\text{Na}_6(\text{THF})_6]\cdot\text{hex}$, **6** $\cdot\text{hex}$. Ellipsoids at 50%. Carbon atoms in gray, C–C bond between reduced imino groups in orange. Solvent molecules and hydrogen atoms omitted for clarity.

moieties through formation of two C–C bonds between the reduced imino carbon atoms of three different ligands. Six sodium cations counterbalance the charge of the complex. In complex **6**, two sodium cations are positioned into the O_4 pockets formed by the phenolate and methoxy groups of the $\text{tris-}^{\text{OME}}\text{salophen}^{10-}$ ligand. The four remaining Na^+ are bound to the phenolate groups and to the amido groups of the ligand. The planarity of the $^{\text{OME}}\text{salophen}^{4-}$ fragment binding the Co(II) cation is distorted in a zigzag fashion compared to the $[\text{Co}^{\text{OME}}\text{salophen}]$ complex due to the presence of the two C–C bonds ($1.586(9)$ Å) connecting this tetra-anionic fragment to the two $^{\text{OME}}\text{salophen}^{3-}$ fragments in the $\text{tris-}^{\text{OME}}\text{salophen}^{10-}$ ligand. Each cobalt center is tetracoordinated by two oxygen and two nitrogen atoms of the $\text{tris-}^{\text{OME}}\text{salophen}^{10-}$ ligand with a distorted square planar geometry. Significantly different average C–N bond distance are found for the imino ($1.358(8)$ Å) and amido ($1.458(8)$ Å) functions.

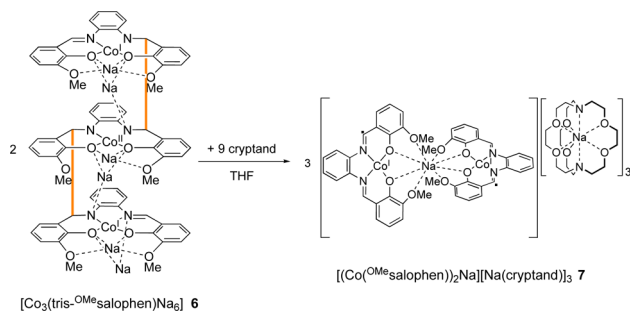
The proton NMR spectra of the crude reaction mixture obtained after addition of 2 equiv of Na to a suspension of Co(II) $[\text{Co}^{\text{OME}}\text{salophen}]$ and of the crystals of **6** both show the presence of two sets of 14 signals between 13 and 2 ppm with integral ratio 2:1. This is in agreement with the presence of two symmetry related $^{\text{OME}}\text{salophen}$ moieties and a third independent $^{\text{OME}}\text{salophen}$ unit as observed in the solid state structure. The same proton NMR spectrum is also obtained for the reaction mixture formed by the reduction of $[\text{Co}_2(\text{bis-}^{\text{OME}}\text{salophen})\text{Na}_2(\text{THF})_4]$ with one equivalent of sodium per cobalt ion. Variable temperature NMR studies from -40 to 60 $^\circ\text{C}$ of a 3.3 mM solution of complex **6** in $\text{THF-}d_8$ do not reveal any change in the ratio of the two sets of 14 signals, but shifts and overlapping of the broad signals. ^1H NMR spectra at variable concentrations from 5 mM to saturation (21.6 mM of Co monomer) of complex **6** in $\text{THF-}d_8$, do not show any equilibrium in solution. These results suggest that the trinuclear structure is maintained in solution without any equilibrium occurring between possible isomeric forms.

The molecular structure of complex **6** shows that the two electron reduction of the $[\text{Co}^{\text{II}}(\text{OMeSalophen})]$ complex does not lead to the reduction of $\text{Co}(\text{II})$ to $\text{Co}(\text{I})$ but results in the formation of a trinuclear $\text{Co}(\text{I})\text{--Co}(\text{II})\text{--Co}(\text{I})$ compound as a result of the reduction of both the ligand and the metal. Notably the six electrons reduction of three $\text{Co}(\text{II})$ complexes yields two $\text{Co}(\text{I})$, while the remaining four electrons are stored in two C--C bonds formed from the reduction of two imino groups.

In order to assess the role of the cation in the formation of complex **6** and to further investigate the stability of the C--C bond we added cryptand to a solution of **6** in THF.

The addition of 6 equiv of cryptand to complex **6** leads to the formation of the dinuclear complex, $[(\text{Co}^{\text{OMeSalophen}})_2\text{Na}][\text{Na}(\text{cryptand})]_3$, complex **7** (Scheme 3). Dark needles suitable

Scheme 3. Cleavage of C–C Bond upon Cryptand Addition



for X-ray diffraction of **7** were obtained by slow diffusion of a solution of 2.2.2-cryptand in THF into a THF solution of **6**. The structure of complex **7** shows the presence of a trianionic cobalt dimer and of three $(\text{Na}(\text{cryptand}))^+$ cations (Figure 9).

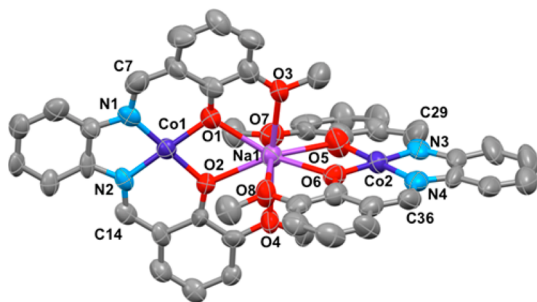


Figure 9. ORTEP of the structure of the $[(\text{Co}^{\text{OMeSalophen}})_2\text{Na}]^{3-}$ anion in **7**. Ellipsoids at 50%. Hydrogen atoms omitted for clarity.

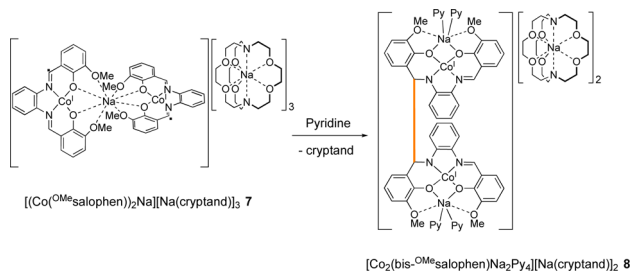
Two $[\text{Co}^{\text{OMeSalophen}}]^{2-}$ moieties in **7** are bridged by a sodium cation in a quasi-perpendicular fashion (85.4° between the planes defined by the N_2O_2 sites of the ligands). The Co atoms are tetracoordinated in a square planar geometry with an average Co--N distance of $1.84(1)$ Å and an average Co--O distance of $1.86(3)$ Å.

The short C--N bond lengths ($1.34(2)$ Å in average) are consistent with the presence of two imino functions on each ligand.

Complex **7** is completely insoluble in THF but soluble in pyridine. However, the ^1H NMR does not show any signal suggesting the presence of fluxional species or free-radical species in solution. Slow diffusion of hexane into a pyridine solution of **7** leads to the isolation of the $\text{Co}(\text{I})$ bis- OMeSalophen dimer $[\text{Co}_2(\text{bis-OMeSalophen})\text{Na}_2\text{Py}_4][\text{Na}(\text{cryptand})]_2$, **8**

(Scheme 4). The solid state structure of complex **8** (see Supporting Information) shows the presence of the hexa-

Scheme 4. Formation of the C–C Bond by Solvent Change



anionic bis- OMeSalophen ligand restored via the formation of a C--C bond ($1.598(13)$ Å) between the two carbon atoms of imino groups from two different $\text{Co}^{\text{OMeSalophen}}$ units. Each cobalt center is tetracoordinated by two oxygens and two nitrogens of the bis- OMeSalophen ligand. Two sodium cations are hexacoordinated by four oxygens of the bis- OMeSalophen ligand and two pyridine nitrogens. The two additional sodium cations are encapsulated by cryptand moieties. The C--N distances found for the imino ($1.350(9)$ Å) and amido ($1.462(9)$ Å) nitrogens are significantly different confirming the presence of double and simple bond, respectively.

These results show that, while it was not possible to identify equilibria between different solution species for **6** in THF, changes in the nature of the cation and in the nature of solvent lead to redistribution of the electrons in the overall structure. This indicates that the two-electrons introduced on the $[\text{Co}^{\text{II}}(\text{OMeSalophen})]$ complex upon reduction by alkali metal in THF can easily redistribute between metal and ligand.

In order to further analyze the structure of these species, EPR spectra were measured for complexes **6** and **7**.

The EPR of a solution of complex **6** in THF/DIPE shows a characteristic signal of a $\text{Co}(\text{II})$ species with a rhombic g tensor and a well-defined hyperfine tensor with the $I = 7/2$ ^{59}Co nuclear spin (Figure 10b). Similarly, the EPR of powdered crystals of complex **6** in hex/DIPE shows a characteristic signal of a $\text{Co}(\text{II})$ species with a rhombic g tensor and a well-defined hyperfine tensor with the $I = 7/2$ ^{59}Co nuclear spin (Figure 10c). Upon closer analysis, it is possible to observe in the EPR spectrum of crystals of **6** the presence of at least one very minor

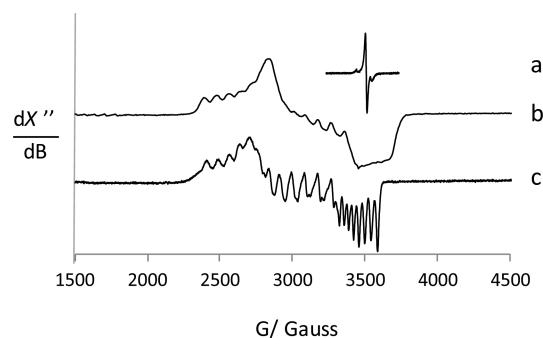


Figure 10. X-Band (9.64 GHz) EPR spectra of (a) powdered $[(\text{Co}^{\text{OMeSalophen}})_2\text{Na}][\text{Na}(\text{cryptand})]_3$ **7**, as a suspension in a mixture 4:1 hex/DIPE at 10K and 32 dB, (b) a solution of $[\text{Co}_3(\text{tris-OMeSalophen})\text{Na}_6(\text{THF})_6]$ **6**, in a mixture 4:1 THF/DIPE at 20K and 23 dB, (c) powdered $[\text{Co}_3(\text{tris-OMeSalophen})\text{Na}_6(\text{THF})_6]$ **6**, as a suspension in a mixture 4:1 hex/DIPE at 20K and 21 dB.

species. These Co(II) impurities are present in sizable quantity in the raw reaction mixture and are gradually removed by successive recrystallization as demonstrated by EPR spectra (see [Supporting Information](#)). The EPR of solutions of **6** shows the presence of the same species, the only difference arising from the broader lines that blur out the smallest hyperfine interactions ([Figure 10b](#)). The origin of this broadening could be the presence of sizable *g* and *A* strain due to slight geometrical changes around the Co(II) ion.

The EPR spectrum at 10 K of the complex **7** isolated by addition of cryptand to a solution of complex **6** in THF does not show any trace of an EPR active Co(II) species. Rather, it consists of a narrow (11 G peak to peak) and nearly isotropic line ($g = 1.968$) that points toward the presence of a paramagnetic species with a strong radical character. This spectrum could be explained by the presence of a low spin Co(I) system with a ligand centered radical. The presence of a Co(0) species can be ruled out by the absence of any sizable hyperfine coupling with the ^{59}Co $I = 7/2$ nuclear spin.^{63,64} Two minor signals can be noted on this spectrum. From batch to batch, the relative intensity of these species changes. They could be due to impurities or to a system with a different electron localization.

Reactivity. Proton NMR studies show that a THF solution of complex **6** reacts readily with 3 equiv of AgOTf affording the Co(I) $[\text{Co}^{\text{OMe}}\text{salophen}]\text{Na}$ complex as the only NMR active product (see [Supporting Information](#)). This suggests that the electrons stored in the C–C bonds are available for the reduction of substrates.

Since the electrons stored in the complexes formed from the reduction of $[\text{Co}^{\text{II}}(\text{OMe}\text{salophen})]$ are easily available at the metal center, we have investigated the possibility of using them for the reductions of carbon dioxide.

The reaction of complex **3** with CO_2 resulted only in the reversible coordination of CO_2 as previously reported for **3** and **4** by Floriani and co-workers.⁵⁷ The exposure of complex **3** to CO_2 (1 atm) in THF- d_8 lead to the formation of a completely insoluble product as previously described. ^1H NMR studies of the reaction of **3** with CO_2 show that the diamagnetic Co(I) complex first reacts with CO_2 followed by complete disappearance of all signals (Co(I) and Co(II)) and formation of an insoluble product. Suspension of this product in THF leads to CO_2 release and restoration of the proton NMR signals of complexes **3**. In contrast complex **6** reacts irreversibly with excess $^{13}\text{CO}_2$ (1 atm) in THF- d_8 to yield a brown suspension. The ^1H NMR spectrum in THF- d_8 of the supernatant after 1 night is NMR silent. Single crystals suitable for X-ray diffraction of the complex $[\text{Co}^{\text{OMe}}\text{salophen-CO}_2]\text{Na}_2[\text{Na}(\text{cryptand})]_2$, **9**, were obtained by slow diffusion of DIPE into a THF solution of **6** reacted with CO_2 after addition of cryptand. The structure of complex **9** shows the presence of the product of ligand-based CO_2 reduction. The structure of complex **9**·(THF)₂ ([Figure 11](#)) is composed of the dimeric dianion $[\text{Co}^{\text{OMe}}\text{salophen-CO}_2]_2\text{Na}_2^{2-}$ and of two $[\text{Na}(\text{cryptand})]^+$ cations. Each Co(II) atoms is tetracoordinated in a square planar geometry by the tetra-anionic $\text{OMe}\text{salophen-CO}_2^{4-}$ ligand resulting from the addition of CO_2 to one imino carbon of the $\text{OMe}\text{salophen}$ ligand. Each Na^+ cation bind a carboxylate and a phenolate from an adjacent $[\text{Co}^{\text{OMe}}\text{salophen-CO}_2]\text{Na}^-$ anion yielding a $[\text{Co}^{\text{OMe}}\text{salophen-CO}_2]_2\text{Na}_2^{2-}$ dianion. A significant lengthening of the C–N bond distances is observed for the CO_2 –C–N bonds (1.456(7) and 1.474(8) Å) compared to the imino C–N bonds (1.302(8) and 1.320(8) Å) in agreement with the

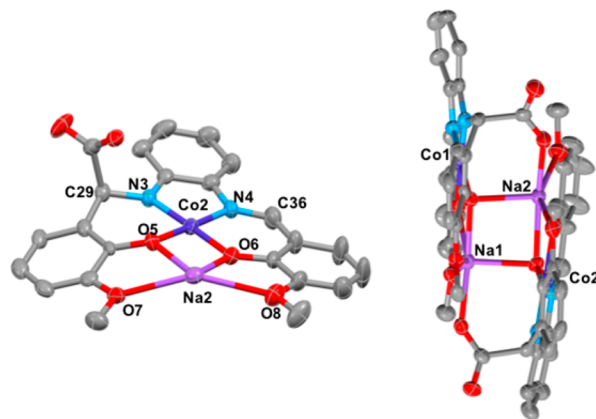


Figure 11. ORTEP of the structure of the dianion $[\text{Co}^{\text{OMe}}\text{salophen-CO}_2]\text{Na}_2^{2-}$ in **9** (right) and of the $[\text{Co}^{\text{OMe}}\text{salophen-CO}_2]\text{Na}^-$ fragment (left). Ellipsoids at 50%. Lattice solvent molecules and hydrogen atoms omitted for clarity.

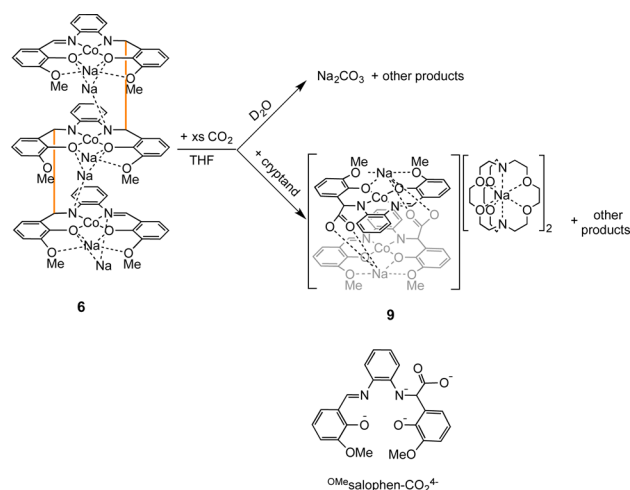
presence of a CO_2 –C–N single bond. The two C–C_{carboxylate} bond lengths found in the dimer are significantly different (1.590(7) Å and 1.556(8) Å) but both comparable to values found for C–C bonds formed from reductive coupling of the salophen imino groups in complexes **4** and **6**. The O–C–O angle values of the carboxylate moieties are 126.4(5)° and 128.9(6)°. The two carboxylate functions feature a slightly longer C–O_{carboxylate} bond distance for the oxygen atoms coordinated to the sodium cation (1.257(6) Å in average) compared to the unbound oxygen atoms (1.230(4) Å in average). However, these C–O distances remain short in agreement with the presence of a delocalized double bond.

Unfortunately, because of the low solubility of **9** and of the presence of multiple reaction products, complex **9** could not be isolated in reasonable amounts for further characterization.

The dissolution in deuterated water of the residue obtained after removal of volatiles from the reaction mixture obtained from the reaction of **6** with excess $^{13}\text{CO}_2$ leads to partial dissolution of the solid. The ^{13}C NMR spectrum of this water solution shows a signal at 167 ppm, assigned to the CO_3^{2-} dianion.⁶⁵ The addition of ^{13}C labeled sodium acetate as internal standard allows the determination of the yield in carbonate product that amounts to 53% of CO_3^{2-} (per Co atom). When only 1 eq of $^{13}\text{CO}_2$ per Co atom is added onto a THF- d_8 solution of **6**, a comparable yield in carbonate was measured (58%). Carbon monoxide should also form in the disproportionation reaction of CO_2 to carbonate, but it could not be observed by ^{13}C NMR spectroscopy probably because of the CO coordination to the cobalt center.⁶⁶ These results show that the electrons stored into the C–C bond become available for the reduction of CO_2 to CO_2^- which subsequently disproportionates to yield carbonate and CO or may add onto the ligand framework ([Scheme 5](#)). The formation of complex **9** may result either from direct two-electron reduction of CO_2 by complex **6** that makes available the two electrons stored in the C–C bonds or by the one electron reduction followed by electrophilic addition to a radical localized on the C–N moiety.

CONCLUSION

To summarize, the one electron reduction of $[\text{Co}^{\text{R}}\text{salophen}]$ with alkali metals leads to the formation of heterometallic Co–M complexes that have undergone either ligand-centered or

Scheme 5. Reaction of Complex 6 with CO₂, and the Ligand ^{OMe}Salophen-CO₂⁴⁻

metal-centered reduction depending on the alkali ion. The two electron reduction of [Co(^Rsalophen)] results in both ligand centered and metal centered reduction affording a Co(I)–Co(II)–Co(I) complex supported by a bridging deca-anionic tris-^{OMe}salophen¹⁰⁻ ligand where three ^{OMe}salophen units are connected by two C–C bonds. In this case the structure of the trimer is maintained in solution. However, the electrons stored in the two C–C bonds may easily become localized on the metal center upon removal of the bound Na cation from the neutral complex [Co₃(tris-^{OMe}salophen)Na₆(THF)₆]. Notably, removal of the cations leads to the cleavage of the C–C bonds and isolation of a new species, [(Co(^{OMe}salophen))₂Na][Na(cryptand)]₃ where the formal oxidation state of the cobalt is (0). The EPR spectrum of this species suggests the presence of Co(I) bound to a radical anion ligand. Thus, these results demonstrated the reversible storage of electrons on redox active ligands bound to cobalt ions and the key role of bound alkali cations in such processes. Moreover, The Co(I)–Co(II)–Co(I) complex reacts with CO₂ in ambient conditions by transferring the electrons stored in the C–C bonds. The reaction results in the formation of carbonate, but also on the addition of the reduced CO₂ onto the ligand framework. These results show that electrons stored in reversible C–C bond may be used for the transformation of carbon dioxide. We anticipate that careful tuning of the ligand and counterion might allow to prevent the addition of the carbon dioxide on the ligand and studies in this direction will be performed in the future.

EXPERIMENTAL SECTION

General Considerations. Unless otherwise noted, all manipulations were carried out at ambient temperature under an inert atmosphere using Schlenk techniques and an MBraun glovebox equipped with a purifier unit. The water and oxygen level were always kept at less than 1 ppm. Glassware was dried overnight at 130 °C before use.

¹H and ¹³C NMR. Experiments were carried out using NMR tubes adapted with J. Young valves. NMR spectra were recorded on Bruker 200 and 400 MHz and on Varian Mercury 400 MHz spectrometers, at various temperatures. NMR chemical shifts are reported in ppm with solvent as internal reference. Diffusion coefficient measurements were performed by NMR using a Pulsed-Field Gradient STimulated Echo (PFGSTE) sequence (see [Supporting Information](#)), using bipolar Gradients, at 298 K and no spinning was applied to the NMR tube.

Elemental Analyses. Analyses were performed under argon by Analytische Laboratorien GMBH at Lindlar, (Germany) or by the elemental analyses department of the EPFL using a Thermo Scientific Flash 2000 Organic Elemental Analyzer.

Starting Materials. Unless otherwise noted, reagents were purchased from commercial suppliers and used without further purification. 2,2,2-Cryptand was recrystallized from THF prior to use. Commercial anhydrous CoCl₂ was purified by extraction in THF to yield CoCl₂(THF)₂. [Co{N(SiMe₃)₂}(THF)] was prepared as previously reported.⁶⁷ The solvents were purchased from Aldrich, Eurisotop or Cortecnet (deuterated solvents) in their anhydrous form, conditioned under argon and vacuum distilled from K/benzophenone (pyridine, DIPE, DME and THF) or sodium dispersion (hexane). All reagents were dried under high-vacuum for 7 days prior to use.

Schiff-base ligands were prepared in air by the condensation of 1,2-phenylenediamine with the corresponding salicylaldehyde derivatives (1:2 stoichiometric ratio) in ethanol under reflux similarly to earlier procedures.⁶⁸

The potassium salts of the Schiff base ligands were prepared as previously described^{42,69} by addition of KH or NaH to a THF solution of the corresponding Schiff base. The resulting M₂^Rsalophen (yellow to orange), salts were obtained in 70–95% yield.

K₂salophen. ¹H NMR (200 MHz, THF-*d*₈, 298 K) δ = 8.4 (s, 2H), 7.2 (s, 2H), 7.1 (s, 2H), 7.0 (s, 2H), 6.8 (s, 2H), 6.4 (s, 2H), 6.1 (s, 2H).

Na₂salophen. ¹H NMR (200 MHz, THF-*d*₈, 298 K) δ = 8.6 (s, 2H), 7.4 (d, 2H), 6.9–7.3 (m, 8H), 6.5 (t, 2H).

K₂^{OMe}salophen. ¹H NMR (200 MHz, DMSO-*d*₆, 298 K) δ = 8.5 (s, 2H), 7.0–6.9 (m, 4H), 6.7 (t, 2H), 6.4 (d, 2H), 5.7 (t, 2H), 3.6 (s, 6H).

Na₂^{OMe}salophen. ¹H NMR (200 MHz, pyridine-*d*₅, 298 K) δ = 8.6 (s, 2H), 7.3 (s, 4H), 7.1 (d, 2H), 6.6 (d, 2H), 6.4 (t, 2H), 3.3 (s, 6H).

Complex Syntheses. [Co(salophen)], and [Co(^{OMe}salophen)] were prepared from CoCl₂·THF according to the published procedure,³⁷ or from addition of protonated H₂salophen/H₂^{OMe}salophen ligand to [Co{N(SiMe₃)₂}(THF)].

[Co(salophen)]K, 1. [CoCl₂(THF)] (551.0 mg, 2.7 mmol, 1 equiv) is added on a suspension of K₂salophen (1.071 g, 2.7 mmol, 1 equiv) in THF (18 mL) and the red suspension was stirred for 5 h at room temperature. Then potassium chunks (106.7 mg, 2.7 mmol, 1 equiv) were added. The mixture was stirred for 24 h affording a brown suspension. A brown precipitate was collected by filtration and dried under vacuum (945.1 mg, 80%). ¹H NMR (400 MHz, THF-*d*₈, 298 K) δ = 10.4 (s, 2H), 7.9 (d, 2H), 7.4 (t, 2H), 7.2 (m, 2H), 6.5 (m, 2H), 6.1 (s, 2H), 5.9 (s, 2H). Anal. Calcd for [Co(salophen)]K(KCl)_{0.33} C₂₀H₁₄N₂O₂CoK_{1.33}Cl_{0.33}: C, 54.97; H, 3.23; N, 6.41, Cl, 2.68. Found: C, 55.14; H, 3.55; N, 6.61; Cl, 4.33. ES-MS *m/z* = 373.2 [M – K]⁺. Single crystals of [Co(salophen)]K(THF) suitable for X-ray diffraction were obtained by slow diffusion of diisopropylether into a THF solution of complex.

[Co(^{OMe}salophen)]K, 2. Potassium chunks (6.5 mg, 0.2 mmol, 1 equiv), was added onto a brown suspension of [Co(^{OMe}salophen)(THF)_{0.5}](KCl)_{0.2} (80.4 mg, 0.2 mmol, 1 equiv) in THF (4 mL). The suspension was stirred 6 days at room temperature affording a greenish suspension. The precipitate was collected by filtration and dried under vacuum (79.0 mg). ¹H NMR (200 MHz, THF-*d*₈, 298 K) δ = 10.3 (s, 2H), 7.5 (d, 2H), 7.2 (s, 2H), 7.0 (s, 2H), 6.6 (s, 2H), 6.0 (s, 2H), 3.6 (s, 6H). Anal. Calcd for [Co(^{OMe}salophen)]K.(THF)_{0.5}(KCl)_{0.02} C₂₄H₂₂N₂O_{4.5}CoK_{1.02}Cl_{0.02}: C, 56.28; H, 4.33; N, 5.47. Found: C, 55.94; H, 3.96; N, 5.11. Single crystals of [Co(^{OMe}salophen)]K(THF) suitable for X-ray diffraction were obtained by slow diffusion of diisopropylether into a THF solution of complex.

[Co₂(bis-salophen)Na₂(THF)₂], 3. Title compound was prepared using a procedure slightly modified with respect to the previously published one³⁷ (in the published procedure an excess sodium is added and the reaction is stopped before all sodium is consumed). [CoCl₂(THF)] (415.4 mg, 2.0 mmol, 1 equiv) is added onto a solution of Na₂salophen (741.3 mg, 2.0 mmol, 1 equiv) in THF (18 mL) and the red suspension is stirred for 5 h at room temperature. Then sodium chunks (46.0 mg, 2.0 mmol, 1 equiv) were added. The

mixture was stirred for 24 h affording a green suspension. The mixture was filtered to remove NaCl and the THF volume of the filtrate was reduced to 3 mL. Slow layering with diisopropylether gave a brown precipitate which was collected by filtration and dried under vacuum (720 mg, 87%). ^1H NMR depends on the concentration. Diluted (0.010 M) ^1H NMR (400 MHz, $\text{THF}-d_8$, 298 K) δ = 10.6 (s, 2H), 7.9 (d, 2H, 3J = 7.2 Hz), 7.4 (t, 2H, 3J = 7.3 Hz), 7.2 (dd, 2H, 3J = 3.3 Hz, 3J = 5.9 Hz), 6.6 (dd, 2H, 3J = 3.3 Hz, 3J = 5.9 Hz), 6.1 (t, 2H, 3J = 7.3 Hz), 6.0 (d, 2H, 3J = 7.2 Hz). Concentrated (0.336 M): apparition of paramagnetic signals ^1H NMR (400 MHz, $\text{THF}-d_8$, 298 K) δ = 48.6 (s, 2H), 29.8 (d, 2H), 18.1 (s, 2H), 13.9 (s, 2H), 4.9 (s, 2H), 1.8 (s, 2H), 0.9 (s, 2H), -3.3 (s, 2H), -5.6 (s, 2H), -8.8 (s, 2H), -16.1 (s, 2H), -28.8 (s, 2H), -59.1 (s, 2H), -124.8 (s, 2H). ES-MS m/z = 373.2 $[\text{Co}(\text{salophen})]^-$, 769.5 $[\text{Co}_2(\text{bis-salophen})\text{Na}]^-$. Anal. Calcd for $[\text{Co}_2(\text{bis-salophen})\text{Na}_2] \cdot (\text{NaCl})_{0.60}$ $\text{C}_{40}\text{H}_{28}\text{N}_4\text{O}_4\text{Co}_2\text{Na}_{2.60}\text{Cl}_{0.60}$ C, 58.05; H, 3.41; N, 6.77. Found: C, 58.11; H, 3.82; N, 6.29.

X-ray studies on single crystals isolated by slow diffusion of hexane into a THF solution confirmed the presence of the previously reported $[\text{Co}_2(\text{bis-salophen})\text{Na}_2(\text{THF})_6]$.³⁷

$[\text{Co}_2(\text{bis-salophen})\text{Li}_2(\text{Py})_4]$, 5. Lithium chunks (2.7 mg, 0.4 mmol, 1 equiv) were added on a solution of $[\text{Co}(\text{salophen})]$ (145.8 mg, 0.4 mmol, 1 equiv) in THF (6 mL). The mixture was stirred for 24 h affording a green solution. The solution was taken to dryness and the obtained residue was crystallized by slow diffusion of hexane into a pyridine solution of the complex (103.9 mg, 70%). ^1H NMR depends on the concentration. Diluted (0.02 M) ^1H NMR (400 MHz, $\text{THF}-d_8$, 298 K) δ = 10.4 (s, 2H), 7.9 (d, 2H), 7.3 (m, 4H), 6.7 (s, 2H), 6.1 (m, 4H). Concentrated (0.34 M) apparition of paramagnetic signals ^1H NMR (400 MHz, $\text{THF}-d_8$, 298 K) δ = 50.8 (s, 2H), 32.8 (s, 2H), 17.9 (s, 2H), 12.6 (s, 2H), 7.5 (s, 2H), 7.0 (s, 2H), 2.4 (s, 2H), -3.5 (s, 2H), -5.6 (s, 2H), -13.0 (s, 2H), -14.0 (s, 2H), -30.0 (s, 2H), -56.9 (s, 2H), -131.5 (s, 2H). Anal. Calcd for $[\text{Co}(\text{salophen})\text{Li}] \cdot (\text{Py})_{1.65}$ $\text{C}_{28.25}\text{H}_{22.25}\text{N}_{3.65}\text{O}_2\text{CoLi}$ C, 66.46; H, 4.39; N, 10.01. Found: C, 66.07; H, 4.44; N, 10.40. Single crystals of $[\text{Co}_2(\text{Py})_2(\text{bis-salophen})\text{Li}_2(\text{Py})_4]$ suitable for X-ray diffraction were obtained by slow diffusion of hexane into a pyridine solution of $[\text{Co}(\text{salophen})\text{Li}]/[\text{Co}_2(\text{bis-salophen})\text{Li}_2]$ mixture.

$[\text{Co}_3(\text{tris-}^{\text{OMe}}\text{salophen})\text{Na}_6(\text{THF})_6]$, 6. $[\text{CoCl}_2(\text{THF})]$ (633.1 mg, 2.9 mmol, 1 equiv) is added onto a suspension of $\text{Na}_2^{\text{OMe}}\text{salophen}$ (1.2 g, 2.9 mmol, 1 equiv) in THF (30 mL) and the resulting brown suspension was stirred for 5 h at 323 K. Then sodium chunks (137.0 mg, 5.8 mmol, 2 equiv) were added. The resulting mixture was stirred for 5 days at room temperature to yield a dark green suspension that was filtered to obtain a green solid after washing with THF. A slow diffusion of hexane into a THF solution of the complex affords $[\text{Co}_3(\text{tris-}^{\text{OMe}}\text{salophen})\text{Na}_6(\text{THF})_6]$ crystals suitable for X-ray diffraction (68% yield). ^1H NMR (400 MHz, $\text{THF}-d_8$, 298 K) δ = 12.8 (s, 2H), 12.5 (br s, 1H), 9.5 (br s, 1H), 9.2 (br s, 1H), 8.6 (d, 2H), 8.5 (br s, 1H), 8.3 (d, 2H), 7.9 (d, 2H), 7.8 (d, 2H), 7.4 (br s, 1H), 7.2 (br s, 1H), 7.0 (s, 2H), 6.7–6.6 (m, 4H), 6.5 (br s, 1H), 6.4 (d, 2H), 6.2 (d, 2H), 6.1 (br s, 1H), 5.9 (t, 2H), 5.3 (t, 2H), 4.9 (br s, 1H), 4.7 (br s, 2H), 4.5 (br s, 1H), 3.4 (s, 6H, CH_3), 3.1 (s, 6H, CH_3), 2.4 (br s, 3H, CH_3), 2.2 (br s, 3H, CH_3). Anal. Calcd for $[\text{Co}_3(\text{tris-}^{\text{OMe}}\text{salophen})\text{Na}_6(\text{THF})_{2.5}] \cdot (\text{NaCl})_{0.3}$ $\text{C}_{76}\text{H}_{74}\text{N}_6\text{O}_{14.5}\text{Co}_3\text{Na}_{6.3}\text{Cl}_{0.3}$ C, 55.81; H, 4.56; N, 5.14. Found: C, 55.55; H, 4.78; N, 4.76.

$[(\text{Co}^{\text{OMe}}\text{salophen})_2\text{Na}][\text{Na}(\text{cryptand})]_3$, 7. A THF (20 mL) solution of cryptand (95.1 mg, 0.2 mmol, 6 equiv) was diffused into a green THF (50 mL) solution of $[\text{Co}_3(\text{tris-}^{\text{OMe}}\text{salophen})\text{Na}_6(\text{THF})_{2.5}] \cdot (\text{NaCl})_{0.3}$ (60.5 mg, 0.04 mmol, 1 equiv) leading to the formation of brown needles (78.6 mg, 68% yield) and suitable for X-ray diffraction. Complex 6 is insoluble in THF which prevent its NMR characterization in this solvent and the ^1H NMR spectrum in deuterated pyridine is silent. Anal. Calcd for $[(\text{Co}^{\text{OMe}}\text{salophen})_2\text{Na}][\text{Na}(\text{cryptand})]_3$ $\text{C}_{98}\text{H}_{144}\text{N}_{10}\text{O}_{26}\text{Co}_2\text{Na}_4$ C, 56.37; H, 6.95; N, 6.71. Found: C, 56.44; H, 6.98; N, 6.46.

Crystals of $[\text{Co}_2(\text{bis-}^{\text{OMe}}\text{salophen})\text{Na}_2\text{Py}_4][\text{Na}(\text{cryptand})]_2$, 8 were isolated by slow diffusion of hexane into a pyridine solution of 7. Complex 8 could not be isolated analytically pure in significant amounts.

Reaction of $[\text{Co}(\text{salophen})\text{K}(\text{THF})]$ with Carbon Dioxide.

$[\text{Co}(\text{salophen})\text{K}] \cdot (\text{KCl})_{0.33}$ (100.0 mg, 0.2 mmol) was dissolved in THF (8 mL) in a J. Young flask under argon. The solution was degassed and an excess of $^{13}\text{CO}_2$ (1 atm) was introduced in the solution. A brown precipitate slowly appeared after 1 h of stirring. The brown precipitate was collected by filtration and dried under vacuum to recover 82 mg of the $[\text{Co}(\text{salophen})\text{K}(\text{CO}_2)(\text{THF})_n]$ complex. The ^1H NMR spectrum taken (400 MHz, $\text{THF}-d_8$, 298 K) recorded for the brown solid dissolved in $\text{THF}-d_8$ showed only the presence of signals assigned to $[\text{Co}(\text{salophen})\text{K}]$. ^{13}C NMR (400 MHz, $\text{THF}-d_8$, 298 K) δ = 125.8 (free $^{13}\text{CO}_2$).

Reaction of $[\text{Co}_3(\text{tris-}^{\text{OMe}}\text{salophen})\text{Na}_6(\text{THF})_6]$, 6 with Carbon Dioxide. $[\text{Co}_3(\text{tris-}^{\text{OMe}}\text{salophen})\text{Na}_6(\text{THF})_{2.5}] \cdot (\text{NaCl})_{0.3}$ (6.3 mg, 0.004 mmol) was dissolved in $\text{THF}-d_8$ (0.5 mL) in a J. Young NMR tube under argon. The solution was degassed and an excess of $^{13}\text{CO}_2$ (approximately 74 equiv) was introduced in the tube. The mixture turned purple instantaneously and then slowly became brown and an important brown precipitate formed. The ^1H NMR spectrum after 1 night does not show any signal. THF was then removed under vacuum and the residue was dried 5 min under dynamic vacuum. $\text{THF}-d_8$ (0.5 mL) was added, the ^1H NMR spectrum remained silent and the ^{13}C NMR spectrum did not show the signal of free $^{13}\text{CO}_2$. THF was removed again and the residue was dried for 30 min under dynamic vacuum. The residue was suspended in D_2O where only a part of the solid dissolves. ^{13}C NMR spectrum (400 MHz, D_2O , 298 K): 167.5 ppm (CO_3^{2-}) shows the presence of carbonate in 53% yield (using ^{13}C labeled sodium acetate as internal standard). A similar yield in carbonate was measured from the reaction of 6 with 3 equiv of CO_2 .

When the reaction's scale was increased to 43.5 mg of complex 6, and an excess of 2.2.2-cryptand was added after the reaction of 6 with excess CO_2 , single crystals of $[\text{Co}^{\text{OMe}}\text{salophen}-\text{CO}_2]\text{Na}_2[\text{Na}(\text{cryptand})]_2$, 9, were obtained by slow diffusion of DIPE into the THF reaction medium.

X-ray Crystallography. Experimental details for X-ray data collections of all complexes are given in Table S1. Figure Graphics are created using MERCURY 3.9 Supplied with Cambridge Structural Database; CCDC: Cambridge, U.K., 2004–2016. Diffraction data of 1, 2, 5 were measured using an Oxford-Diffraction XCalibur S at low temperature [150(2) K] The data sets were reduced by CrysAlis (CrysAlisPro, Rigaku Oxford Diffraction) and then corrected for absorption.⁷⁰ The diffraction data of 6 and 8 were measured at low temperature [100(2) K] using Mo $K\alpha$ radiation on a Bruker APEX II CCD diffractometer equipped with a kappa geometry goniometer. The data sets were reduced by EvalCCD⁷¹ and then corrected for absorption.⁷² The data collection of compounds 7 and 9 were performed at low temperature [140(2) K] using Cu $K\alpha$ (7) or Mo $K\alpha$ (9) radiation on a Rigaku SuperNova dual system in combination with an Atlas CCD detector. The data reduction was carried out by CrysAlis PRO.⁷⁰ The solutions and refinements were performed by SHELXT and SHELXL.⁷³ The crystal structures were refined using full-matrix least-squares based on F^2 with all non hydrogen atoms anisotropically defined. Hydrogen atoms have been located in calculated positions by means of the "riding" model. Additional electron density found in the difference Fourier map (due to highly disordered solvent) of 6 and 7 was treated by the SQUEEZE algorithm of PLATON.⁷⁴

EPR Measurements. EPR experiments were carried out using 4 mm EPR tubes adapted with J. Young valves. Solid samples were carefully ground before the measurements. EPR of the solutions at different concentrations were recorded after rapidly freezing the solutions after equilibrium was reached at 298 K. EPR spectra were recorded on a Bruker EMX continuous wave spectrometer operating at X band frequency equipped with an Oxford instrument ESR 900 Helium flow cryostat. For each experiment, magnetic field was recorded with a Bruker Gaussmeter ER035 M and microwave frequency was recorded with an Hewlett-Packard Microwave Frequency Counter 5350B.

■ ASSOCIATED CONTENT

● Supporting Information

The Supporting Information is available free of charge on the ACS Publications website at DOI: [10.1021/jacs.7b03604](https://doi.org/10.1021/jacs.7b03604).

¹H NMR and EPR spectra (PDF)

X-ray crystallographic data for complex 2 (CIF)

X-ray crystallographic data for complex 1 (CIF)

X-ray crystallographic data for complex 5 (CIF)

X-ray crystallographic data for complex 7 (CIF)

X-ray crystallographic data for complex 6 (CIF)

X-ray crystallographic data for complex 9 (CIF)

X-ray crystallographic data for complex 8 (CIF)

■ AUTHOR INFORMATION

Corresponding Author

*marinella.mazzanti@epfl.ch

ORCID

Marinella Mazzanti: [0000-0002-3427-008X](https://orcid.org/0000-0002-3427-008X)

Notes

The authors declare no competing financial interest.

■ ACKNOWLEDGMENTS

We thank F. Fadaei Tirani for her contribution to the X-ray single crystal structure analyses and E. Solari for the determination of the elemental analyses. We thank D. Toniolo for performing some NMR measurements. We acknowledge support from the Swiss National Science Foundation (200021_157158) and from the Ecole Polytechnique Fédérale de Lausanne (EPFL).

■ REFERENCES

- Luca, O. R.; Crabtree, R. H. *Chem. Soc. Rev.* **2013**, *42*, 1440.
- Lyaskovskyy, V.; de Bruin, B. *ACS Catal.* **2012**, *2*, 270.
- Chirik, P. J. *Inorg. Chem.* **2011**, *50*, 9737.
- Anderson, N. H.; Odoh, S. O.; Yao, Y. Y.; Williams, U. J.; Schaefer, B. A.; Kiernicki, J. J.; Lewis, A. J.; Goshert, M. D.; Fanwick, P. E.; Schelter, E. J.; Walensky, J. R.; Gagliardi, L.; Bart, S. C. *Nat. Chem.* **2014**, *6*, 919.
- Pankhurst, J. R.; Bell, N. L.; Zegke, M.; Platts, L. N.; Lamfsus, C. A.; Maron, L.; Natrajan, L. S.; Sproules, S.; Arnold, P. L.; Love, J. B. *Chem. Sci.* **2017**, *8*, 108.
- Camp, C.; Mougél, V.; Horeglad, P.; Pecaut, J.; Mazzanti, M. J. *Am. Chem. Soc.* **2010**, *132*, 17374.
- Dzik, W. I.; van der Vlugt, J. I.; Reek, J. N. H.; de Bruin, B. *Angew. Chem., Int. Ed.* **2011**, *50*, 3356.
- Chirik, P. J.; Wieghardt, K. *Science* **2010**, *327*, 794.
- Broere, D. L. J.; Plessius, R.; van der Vlugt, J. I. *Chem. Soc. Rev.* **2015**, *44*, 6886.
- Chirik, P. J. *Acc. Chem. Res.* **2015**, *48*, 1687.
- Knijnenburg, Q.; Gambarotta, S.; Budzelaar, P. H. M. *J. Chem. Soc.-Dalton Trans.* **2006**, 5442.
- Bowman, A. C.; Milsman, C.; Atienza, C. C. H.; Lobkovsky, E.; Wieghardt, K.; Chirik, P. J. *J. Am. Chem. Soc.* **2010**, *132*, 1676.
- Anderson, N. H.; Odoh, S. O.; Williams, U. J.; Lewis, A. J.; Wagner, G. L.; Pacheco, J. L.; Kozimor, S. A.; Gagliardi, L.; Schelter, E. J.; Bart, S. C. *J. Am. Chem. Soc.* **2015**, *137*, 4690.
- Thammayongsy, Z.; Seda, T.; Zakharov, L. N.; Kaminsky, W.; Gilbertson, J. D. *Inorg. Chem.* **2012**, *51*, 9168.
- Benson, E. E.; Sampson, M. D.; Grice, K. A.; Smieja, J. M.; Froehlich, J. D.; Friebe, D.; Keith, J. A.; Carter, E. A.; Nilsson, A.; Kubiak, C. P. *Angew. Chem., Int. Ed.* **2013**, *52*, 4841.
- Arana, C.; Yan, S.; Keshavarz, M.; Potts, K. T.; Abruna, H. D. *Inorg. Chem.* **1992**, *31*, 3680.
- Chiericato, G.; Arana, C. R.; Casado, C.; Cuadrado, I.; Abruna, H. D. *Inorg. Chim. Acta* **2000**, *300*, 32.
- Elgrishi, N.; Chambers, M. B.; Artero, V.; Fontecave, M. *Phys. Chem. Chem. Phys.* **2014**, *16*, 13635.
- Lacy, D. C.; McCrory, C. C. L.; Peters, J. C. *Inorg. Chem.* **2014**, *53*, 4980.
- Haneline, M. R.; Heyduk, A. F. *J. Am. Chem. Soc.* **2006**, *128*, 8410.
- King, E. R.; Betley, T. A. *J. Am. Chem. Soc.* **2009**, *131*, 14374.
- Booth, C. H.; Walter, M. D.; Kazhdan, D.; Hu, Y. J.; Lukens, W. W.; Bauer, E. D.; Maron, L.; Eisenstein, O.; Andersen, R. A. *J. Am. Chem. Soc.* **2009**, *131*, 6480.
- Trifonov, A. A.; Borovkov, I. A.; Fedorova, E. A.; Fukin, G. K.; Larionova, J.; Druzhkov, N. O.; Cherkasov, V. K. *Chem. - Eur. J.* **2007**, *13*, 4981.
- Trifonov, A. A.; Shestakov, B. G.; Lyssenko, K. A.; Larionova, J.; Fukin, G. K.; Cherkasov, A. V. *Organometallics* **2011**, *30*, 4882.
- Walter, M. D.; Berg, D. J.; Andersen, R. A. *Organometallics* **2007**, *26*, 2296.
- Waldie, K. M.; Ramakrishnan, S.; Kim, S.; Maclaren, J. K.; Chidsey, C. E. D.; Waymouth, R. M. *J. Am. Chem. Soc.* **2017**, *139*, 4540.
- Booth, C. H.; Kazhdan, D.; Werkema, E. L.; Walter, M. D.; Lukens, W. W.; Bauer, E. D.; Hu, Y. J.; Maron, L.; Eisenstein, O.; Head-Gordon, M.; Andersen, R. A. *J. Am. Chem. Soc.* **2010**, *132*, 17537.
- Schultz, M.; Boncella, J. M.; Berg, D. J.; Tilley, T. D.; Andersen, R. A. *Organometallics* **2002**, *21*, 460.
- Nocton, G.; Lukens, W. W.; Booth, C. H.; Rozenel, S. S.; Medling, S. A.; Maron, L.; Andersen, R. A. *J. Am. Chem. Soc.* **2014**, *136*, 8626.
- Schelter, E. J.; Wu, R. L.; Scott, B. L.; Thompson, J. D.; Cantat, T.; John, K. D.; Batista, E. R.; Morris, D. E.; Kiplinger, J. L. *Inorg. Chem.* **2010**, *49*, 924.
- Monreal, M. J.; Diaconescu, P. L. *J. Am. Chem. Soc.* **2010**, *132*, 7676.
- Nocton, G.; Ricard, L. *Chem. Commun.* **2015**, *51*, 3578.
- Bachmann, J.; Nocera, D. G. *J. Am. Chem. Soc.* **2005**, *127*, 4730.
- Hulley, E. B.; Wolczanski, P. T.; Lobkovsky, E. B. *J. Am. Chem. Soc.* **2011**, *133*, 18058.
- Carmen, C.; Atienza, H.; Milsman, C.; Semproni, S. P.; Turner, Z. R.; Chirik, P. J. *Inorg. Chem.* **2013**, *52*, 5403.
- Liu, B.; Yoshida, T.; Li, X. F.; Stepien, M.; Shinokubo, H.; Chmielewski, P. J. *Angew. Chem., Int. Ed.* **2016**, *55*, 13142.
- DeAngelis, S.; Solari, E.; Gallo, E.; Floriani, C.; ChiesiVilla, A.; Rizzoli, C. *Inorg. Chem.* **1996**, *35*, 5995.
- Franceschi, F.; Solari, E.; Scopelliti, R.; Floriani, C. *Angew. Chem., Int. Ed.* **2000**, *39*, 1685.
- Floriani, C.; Solari, E.; Franceschi, F.; Scopelliti, R.; Belanzoni, P.; Rosi, M. *Chem. - Eur. J.* **2001**, *7*, 3052.
- Solari, E.; Maltese, C.; Franceschi, F.; Floriani, C.; ChiesiVilla, A.; Rizzoli, C. *J. Chem. Soc., Dalton Trans.* **1997**, 2903.
- Gambarotta, S.; Mazzanti, M.; Floriani, C.; Zehnder, M. *J. Chem. Soc., Chem. Commun.* **1984**, *0*, 1116.
- Camp, C.; Andrez, J.; Pecaut, J.; Mazzanti, M. *Inorg. Chem.* **2013**, *52*, 7078.
- Camp, C.; Guidal, V.; Biswas, B.; Pecaut, J.; Dubois, L.; Mazzanti, M. *Chem. Sci.* **2012**, *3*, 2433.
- Isse, A. A.; Gennaro, A.; Vianello, E.; Floriani, C. *J. Mol. Catal.* **1991**, *70*, 197.
- Chen, H. Y.; Sun, Z. J.; Ye, S.; Lu, D. P.; Du, P. W. *J. Mater. Chem. A* **2015**, *3*, 15729.
- Gambarotta, S.; Arena, F.; Floriani, C.; Zanazzi, P. F. *J. Am. Chem. Soc.* **1982**, *104*, 5082.
- Hammouche, M.; Lexa, D.; Momenteau, M.; Saveant, J. M. *J. Am. Chem. Soc.* **1991**, *113*, 8455.
- Jeoung, J. H.; Dobbek, H. *Science* **2007**, *318*, 1461.
- Benson, E. E.; Kubiak, C. P.; Sathrum, A. J.; Smieja, J. M. *Chem. Soc. Rev.* **2009**, *38*, 89.

- (50) Krogman, J. P.; Foxman, B. M.; Thomas, C. M. *J. Am. Chem. Soc.* **2011**, *133*, 14582.
- (51) Cooper, O.; Camp, C.; Pécaut, J.; Kefalidis, C. E.; Maron, L.; Gambarelli, S.; Mazzanti, M. *J. Am. Chem. Soc.* **2014**, *136*, 6716.
- (52) Kilpatrick, A. F. R.; Cloke, F. G. N. *Chem. Commun.* **2014**, *50*, 2769.
- (53) Bagherzadeh, S.; Mankad, N. P. *J. Am. Chem. Soc.* **2015**, *137*, 10898.
- (54) Machan, C. W.; Kubiak, C. P. *J. Chem. Soc.-Dalton Trans.* **2016**, *45*, 15942.
- (55) Kiernicki, J. J.; Ferrier, M. G.; Pacheco, J. S. L.; La Pierre, H. S.; Stein, B. W.; Zeller, M.; Kozimor, S. A.; Bart, S. C. *J. Am. Chem. Soc.* **2016**, *138*, 13941.
- (56) Fachinetti, G.; Floriani, C.; Zanazzi, P. F. *J. Am. Chem. Soc.* **1978**, *100*, 7405.
- (57) Fachinetti, G.; Floriani, C.; Zanazzi, P. F.; Zanzari, A. R. *Inorg. Chem.* **1979**, *18*, 3469.
- (58) Pahor, N. B.; Calligaris, M.; Delise, P.; Dodic, G.; Nardin, G.; Randaccio, L. *J. Chem. Soc., Dalton Trans.* **1976**, 2478.
- (59) Arora, H.; Philouze, C.; Jarjays, O.; Thomas, F. *J. Chem. Soc.-Dalton Trans.* **2010**, *39*, 10088.
- (60) Dugan, T. R.; Bill, E.; MacLeod, K. C.; Christian, G. J.; Cowley, R. E.; Brennessel, W. W.; Ye, S.; Neese, F.; Holland, P. L. *J. Am. Chem. Soc.* **2012**, *134*, 20352.
- (61) Neumann, W. P.; Uzick, W.; Zarkadis, A. K. *J. Am. Chem. Soc.* **1986**, *108*, 3762.
- (62) Wittman, J. M.; Hayoun, R.; Kaminsky, W.; Coggins, M. K.; Mayer, J. M. *J. Am. Chem. Soc.* **2013**, *135*, 12956.
- (63) Deblon, S.; Liesum, L.; Harmer, J.; Schonberg, H.; Schweiger, A.; Grutzmacher, H. *Chem. - Eur. J.* **2002**, *8*, 601.
- (64) Pilloni, G.; Toffoletti, A.; Bandoli, G.; Longato, B. *Inorg. Chem.* **2006**, *45*, 10321.
- (65) Stueber, D.; Patterson, D.; Mayne, C. L.; Orendt, A. M.; Grant, D. M.; Parry, R. W. *Inorg. Chem.* **2001**, *40*, 1902.
- (66) Isse, A. A.; Gennaro, A.; Vianello, E.; Floriani, C. *J. Mol. Catal.* **1991**, *70*, 197.
- (67) Bryan, A. M.; Long, G. J.; Grandjean, F.; Power, P. P. *Inorg. Chem.* **2013**, *52*, 12152.
- (68) Chen, H. Y.; Cronin, J. A.; Archer, R. D. *Inorg. Chem.* **1995**, *34*, 2306.
- (69) Mazzanti, M.; Gambarotta, S.; Floriani, C.; Chiesivilla, A.; Guastini, C. *Inorg. Chem.* **1986**, *25*, 2308.
- (70) *CrysAlisPRO Rigaku Oxford Diffraction*, 2015.
- (71) Duisenberg, A. J. M.; Kroon-Batenburg, L. M. J.; Schreurs, A. M. *J. Appl. Crystallogr.* **2003**, *36*, 220.
- (72) Blessing, R. H. *Acta Crystallogr., Sect. A: Found. Crystallogr.* **1995**, *51*, 33.
- (73) Sheldrick, G. M. *Acta Crystallogr., Sect. C: Struct. Chem.* **2015**, *71*, 3.
- (74) PLATON; Spek, A. L. *Acta Crystallogr., Sect. C: Struct. Chem.* **2015**, *71*, 9.